EasyChair Preprint

№ 11259

A Novel Structure of LLC Integrated Planar Transformer for E-Bike Charger Application

Xuan Phuc Luong, Quang Huy Nguyen, Thanh Hai Phan and Duy Dinh Nguyen

November 7, 2023

A novel structure of LLC integrated planar transformer for e-bike charger applications

Xuan-Phuc Luong
School of Electrical and Electronic Engineering
Hanoi University of Science and Technology
Hanoi, Vietnam
phuc.lx192024@sis.hust.edu.vn

Quang-Huy Nguyen
School of Electrical and Electronic Engineering
Hanoi University of Science and Technology
Hanoi, Vietnam
huy.nq181528@sis.hust.edu.vn

Thanh-Hai Phan
School of Electrical and Electronic Engineering
Hanoi University of Science and Technology
Hanoi, Vietnam
hai.pt181456@sis.hust.edu.vn

Duy-Dinh Nguyen
School of Electrical and Electronic Engineering
Hanoi University of Science and Technology
Hanoi, Vietnam
dinh.nguyenduy@hust.edu.vn

***Abstract*—The LLC resonant converter is one of the most popular isolated DC/DC converters in E-bike charger applications due to its simple control, wide voltage gain regulation capability, soft switching operation, and high power density. The synchronous rectification (SR) technology is applied in the converter, where the secondary side diodes are replaced with SR MOSFETs, considerably reducing the conduction loss of the secondary rectifier, and improving the system efficiency. Additionally, using a planar transformer for the converter helps achieve a low-profile configuration, high power density, and good heat dissipation capability. For 12V power charger applications, using low-voltage SR-MOSFETs offers the advantage of low ON-resistance, reducing terminal losses. However, for power charger applications from 60 - 70V, the current driving ICs are limited and the use of low-voltage SR-MOSFETs is no longer suitable due to the limitation of the breakdown voltage of switches. Therefore, in this paper, a new structure of LLC integrated transformer with planar cores is proposed for E-bike chargers with high output voltage (60 - 70V) that still uses low-voltage integrated SR-MOSFETs and driving integrated circuits (ICs). The proposed transformer has a very compact structure consisting of an integrated resonant inductor, SR MOSFETs, and output capacitors. An 800W LLC resonant converter prototype for E-bike charger applications was designed and tested.**

Keywords—e-bike charger, LLC converter, planar transformer, SR MOSFET.

I. INTRODUCTION

E-bikes are bicycles that can reduce greenhouse gas emissions, improve cardiovascular health, and increase energy efficiency by using a battery-powered motor that assists the rider's pedaling [1]. Among the DC/DC converters used in Ebike battery chargers, LLC converters are attractive due to their advantages, such as working with a wide range of loads, having a wide range of output voltage variations, and soft switching capability that reduces switching loss on the switches, thereby achieving high system efficiency. To further increase the efficiency of the LLC converter, synchronous rectification (SR) technology must be applied. Due to the low on-resistance of SR MOSFET, a considerable reduction in conduction loss of the secondary rectifier can be achieved, thus improving system efficiency.

In high-frequency LLC resonant converters, magnetic components are usually the bulkiest components and determine the overall height of the converter. Due to the height of traditional transformer cores, the shape of LLC converters is often bulky and cumbersome. To implement slim configuration converters for the above applications, planar transformers (PT) utilizing PCB windings can be used. The advantages of planar transformers in DC/DC converters are low profile, good heat dissipation capability, high repeatability, and easy interleaving winding to reduce leakage inductance and AC resistance.

Mounting synchronous rectifier (SR) MOSFET devices on the PCB is an effective way to reduce secondary side winding loss and terminal loss. To reduce the terminal loss and the secondary winding loss, SR-MOSFET and a 3D Planar-Litz winding method are used on the secondary side in [2]. However, the use of Planar-Litz winding leads to losses on the vias, difficulties in designing a PCB layout, and limitations on the number of secondary turns. In papers [3] and [4], transformers with integrated SR-MOSFET and parallel secondary windings are used to reduce the terminal loss and the secondary winding loss. However, both papers are applied to chargers with low output voltage (12V). Therefore, the SR-MOSFETs and the driving ICs used are low-voltage devices unsuitable for E-bike chargers with higher output voltage such as 60V to 70V. To reduce the number of output rectifier switches, the center-taped transformer is often used. With this structure, the break-down voltage of the switch should be chosen to be larger than twice the output voltage. Therefore, in applications with output voltage from 60V to 70V, the break-down voltage of the rectifier switch should be up to 200V.

This paper proposes a new transformer structure for E-bike chargers with high output voltage (60 - 70V) that still uses low-voltage integrated SR-MOSFET and driving ICs by using series-connected secondary windings. Besides integrating SR-MOSFETs to reduce the terminal loss and the size, the proposed transformer uses an interleaving winding structure to reduce the transformer winding loss. The proposed transformer structure comprises an integrated resonant inductor, output capacitors, SR-MOSFETs, and driving ICs. An 800W LLC resonant converter prototype for e-bike applications was designed and tested.

II. PLANAR TRANSFORMER BACKGROUND

This section explains in detail the design considerations for the proposed high-frequency planar transformer structure. These considerations include AC resistance, interleaving windings, and transformer core loss.

Winding losses in transformers dramatically increase with high frequency due to eddy current effects. Eddy current effects

cause the current density to be nonuniform in the cross-section of the conductor and thus cause a higher winding resistance at higher frequency. Based on Dowell's assumptions and the general field solutions for the distribution of current density in a single layer of an infinitely foil conductor, the expression for the AC resistance of the mth layer is derived as follows [5]:

$$\frac{R_{ac,m}}{R_{dc,m}} = \frac{\varepsilon}{2}\left[\frac{\sinh\varepsilon + \sin\varepsilon}{\cosh\varepsilon - \cos\varepsilon} + (2m - 1)^2 \frac{\sinh\varepsilon - \sin\varepsilon}{\cosh\varepsilon + \cos\varepsilon}\right] \quad (1)$$

where $\varepsilon = h/\delta$ is an effective thickness of the skin depth, h is the thickness of the conductor, and δ is the skin depth at a given frequency. The variable m represents a winding portion and defined as a ratio:

$$m = \frac{F(h)}{F(h) - F(0)} \quad (2)$$

where $F(0)$ and $F(h)$ are the MMFs at the limits of a layer surface.

Not all the magnetic flux generated by AC current excitation on the primary side follows the magnetic circuit and link with the secondary winding. The flux linkage between two windings or parts of the same winding is never complete. Some flux leaks from the core and returns to the air, winding layers, and insulator layers; thus, these flux causes imperfect coupling. The leakage inductance based on the 1-D assumption is calculated by calculating the leakage energy (3) and according to analytical MMF distribution.

$$E_{lk} = \frac{\mu_0}{2}\sum \int_0^h H^2 \cdot l_w \cdot b_w \cdot dx \quad (3)$$

where l_w is the length of each turn, b_w is the width of each turn, and h represents the thickness of each winding layer. The field strength H depends on the number of ampere-turns linked by the leak flux path, and thus it depends on the magnetomotive force (MMF) distributions. Figure 2 shows the interleaved winding structure between primary side winding (P), and secondary side winding (S), and thus, MMF distributions of the winding structure are constructed. The interleaved winding technology is commonly used to minimize the leakage inductance in planar magnetics, which can also reduce the winding loss at the same time.

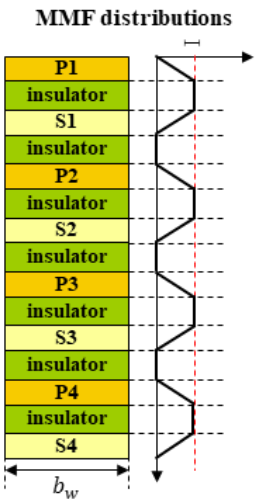

Fig. 1. MMF distributions with interleaving arrangement.

The power loss is the primary consideration during the transformer design process. Basically, the total loss consists of the core loss and the winding loss. According to the maximum flux density, the iGSE equation [6] will be applied to get the core loss shown as:

$$P_{fe} = \frac{1}{T}\int_0^T K_{ic}\left|\frac{dB}{dt}\right|^{\alpha} |B(t)|^{\beta-\alpha} dt \quad (4)$$

with

$$K_{ic} = \frac{K_c}{(2\pi)^{\alpha-1}\int_0^{2\pi}|\cos\theta|^{\alpha}|\sin\theta|^{\beta-\alpha}d\theta} \quad (5)$$

where K_c, α and β are the Steinmetz coefficients, $B(t)$ is the instantaneous flux density.

III. The Proposed Transformer Structure

The LLC resonant converter circuit diagram is shown in Figure 2. The structure of the converter includes a primary side H-bridge inverter, a resonant tank, a center-tap transformer, SR-MOSFETs and output capacitors. The proposed transformer structure consists of two parts: a planar transformer and a planar inductor. An inductor PCB winding is included with the planar core to integrate the resonant inductance of the LLC converter. The designed PCB winding includes 4 conductor layers, insulated from each other by the FR4 substrate layer. The structure of a PCB transformer winding is shown in Figure 3, including the primary winding connected in series designed on two inner layers and each secondary winding located on each outer layer of the PCB. In addition, an SR MOSFET, a gate driver circuit, and output capacitors are integrated into each outer layer of the PCB winding to reduce the size and minimize terminal loss. The primary and secondary windings on each PCB winding are arranged alternately in the SPPS structure. When joining the PCB windings together, the primary windings on each PCB winding are connected in series, the corresponding secondary windings are connected in series. Thus, by joining multiple PCB windings together, the total output voltage across the secondary winding does not change and the voltage drop

across each of these windings is evenly distributed. This helps to reduce the voltage stress on each SR mosfet and gate driver ic, helping to solve the problem of high output voltage. In addition, the structure of the inductor winding on the PCB winding is shown in Figure 4.

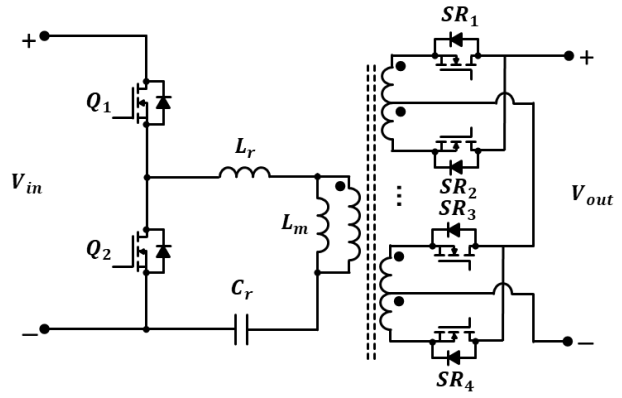

Fig. 2. The LLC resonant converter circuit diagram.

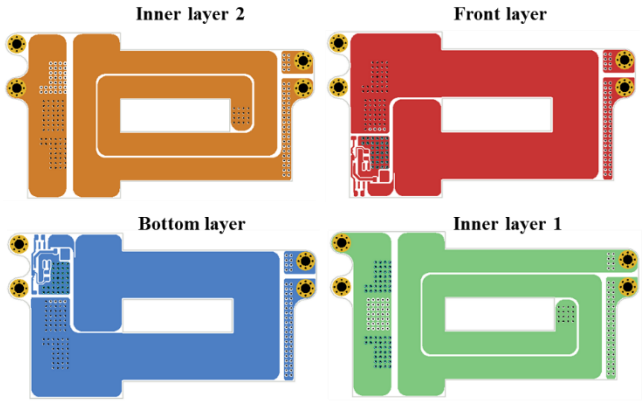

Fig. 3. The primary side and secondary side PCB winding.

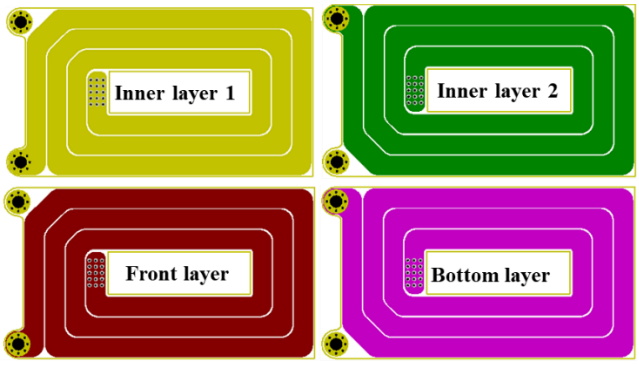

Fig. 4. The inductor PCB winding.

IV. Design and Experimental Results

A. Design specifications

A regulated 400V/60V 800W LLC resonant converter with a planar transformer is established. The normal input voltage range is 350V~400V and the normal output voltage range is 50V~67V. The resonant frequency of the transformer is designed to be 240 kHz.

Table I shows the key parameters for the 800W LLC resonant converter design. In particular, a center taped transformer is used consisting of 3 windings with the ratio of turns being 16: 4: 4.

TABLE I. Key Parameters

Parameters	***Symbol***	**Value**
Resonant capacitor	C_r	25 nF
Resonant inductor	L_r	17.61 µH
Resonant frequency	f_r	240 kHz
Magnetizing inductance of the transformer	L_m	92.8 µH
Transformer turns ratio	$N_p: N_{s1}: N_{s2}$	16: 4: 4

Table II shows the key components used in the 800W LLC resonant converter design.

TABLE II. Key Components

Components	
GaN FETs Q1 and Q2	AON6276
Secondary synchronous rectifier, SR1 ~ SR 8	AON6276
Secondary synchronous rectifier driver	ZXGD3105N8
Integerated transformer cores	ELP43/10/28 x3

Figure 5 shows the proposed planar transformer structure. The integrated transformer has three planar cores with four PCB windings for the transformer and one PCB winding for the resonant inductor. To reduce the DC resistance, the winding of the inductor consists of two parallel layers to increase the cross-section area of the wire. Each layer of inductor winding consists of 3 turns of wire. Therefore, the total number of turns on the inductor is 6 turns. Each transformer PCB winding consists of a secondary winding on each outer layer and four primary windings on the two inner layers. Thus, the winding ratio on one transformer PCB winding is 4:1:1. With this design that has a winding ratio of 16:4:4, the transformer used four PCBs connected together.

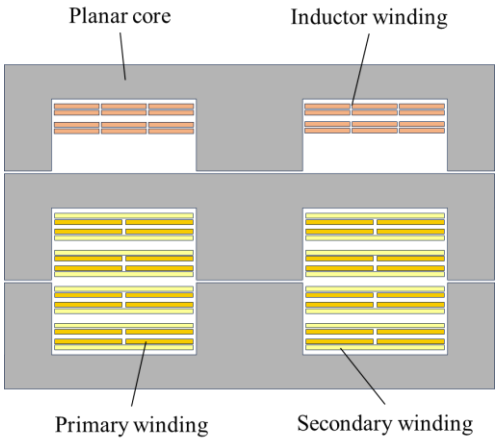

Fig. 5. Intergrated transformer for LLC resonant converter.

The resonant inductor and the transformer share the same magnetic core. Because of the low reluctance path provided by the core with high permeability, the flux generated by the resonant inductor and the transformer will follow the low reluctance path instead of the high reluctance path with air gaps, and thus the resonant inductor and the transformer will not be magnetically coupled. The flux of the resonant inductor will vary with the primary current and the flux between the transformer and the resonant inductor may also be partially cancelled.

B. Simulation and Experimental Results

Before conducting experiments, a finite-element analysis (FEA) using the Finite-Element-Method- magnetic (FEMM) version 4.2 [7] was carried out to validate the designed transformers. The flux density at the inductor core obtained by the FEA is illustrated in Figure 6. The peak flux density at the core is 13.5 mT, which is 5.3% greater than the estimation value.

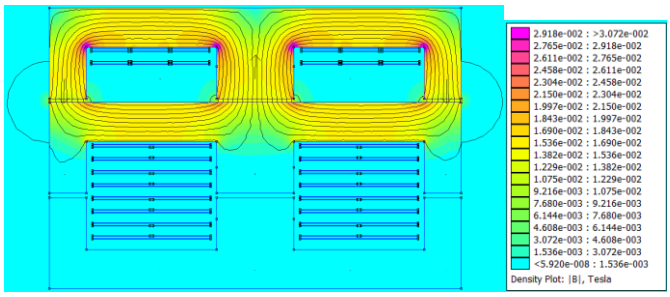

Fig. 6. Simulated flux density of inductor core using FEMM 4.2.

The flux density at the transformer core obtained by the FEA is illustrated in Figure 7. The peak flux density at the core is 166.17 mT, which is 2.6% greater than the estimation value. Except for that, other parameters including leakage inductance, AC resistance, and copper losses are almost identical to the designed values.

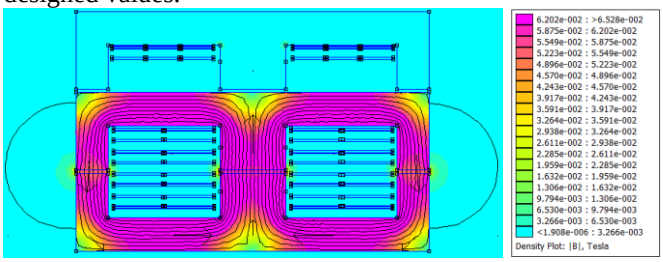

Fig. 7. Simulated flux density of transformer core using FEMM 4.2.

A detailed comparison between calculations, Finite-element analysis (FEA) results, and measurements is given in Table III. It can be seen that measurements matched calculation and FEA results very well. The prediction of transformer loss was also very close to the FEA simulation results.

The estimated power loss break down of 800W load condition is shown in Figure 8.

TABLE III. DESIGN VALIDATION

Parameters	***Calculation***	***FEA***	***Measurement***
Resonant inductance, L_r	17.61	17.23	16.49
Magnetizing inductance of the transformer, L_m	92.80	92.60	92.10
AC resistance of the transformer, $R_{ac,tran}$ [mΩ]	240.05	239.40	291.00
AC resistance of the inductor, $R_{ac,ind}$ [mΩ]	23.05	23.06	123
Peak flux density of the transformer core, $B_{pk,tran}$ [mT]	161.94	166.17	
Copper loss, ΔP_{Cu} [W]	31.49	32.26	

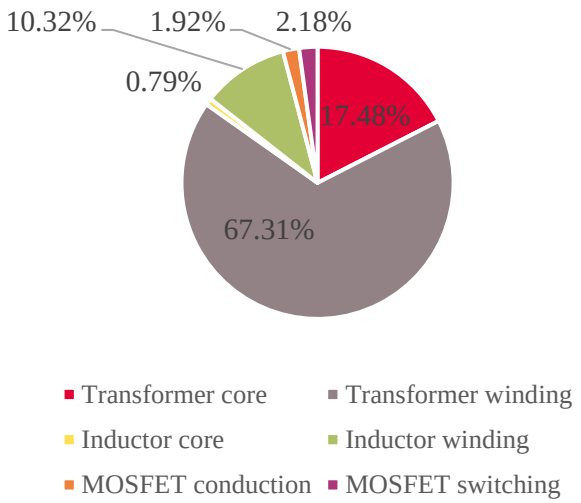

Fig. 8. Power loss break down at 800W Load.

Figure 9 shows the prototype of 800W LLC integrated planar transformer including resonant inductor, integrated transformer with SR-MOSFET AON6276, synchronous rectifier driver ZXGD3105N8 and output capacitors.

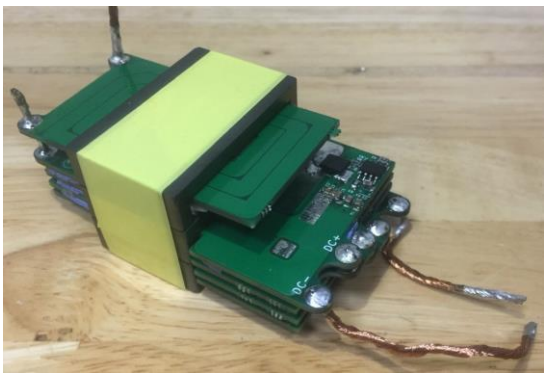

Fig. 9. 800W LLC integrated planar transformer prototype.

Figure 10 shows the measured efficiency and the estimated efficiency for different loads. The measured peak efficiency is 97.42% around 300W and light load and full load efficiency is higher than 94.5%. However, the converter performance is not as good as estimated efficiency. The reason may be due to the increment of drain-source resistance of MOSFETs when

temperature changes, which was not regarded in the loss model above. Another reason is the mismatch of actual parameters of the real, hand-made transformers when compared to the ideal values. Voltage drops on cables connecting input and output of the converter to the power supply and load also contribute to the error between modeling and experiment.

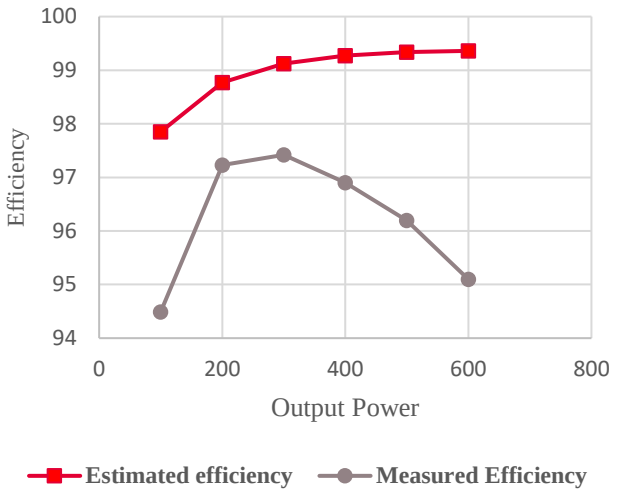

Fig. 10. Measured and estimated efficiency of LLC resonant converter.

V. Conclusion

In this paper, a novel LLC integrated transformer structure for E-bike charger application is proposed. The two main characteristics of this transformer structure are: the interleaving structure of the transformer primary and secondary winding and the winding, rectifier integration technique. The advantages of this structure are:

1. Interleaving structure dramatically reduced the transformer's AC winding losses.
2. The secondary winding structure allows the transformer to be applied in high-voltage chargers (48V - 60V) while using low-voltage SR-MOSFETs and driving ICs.

A 800W LLC integrated transformer prototype employed the proposed transformer structure is constructed, and over 96% converter efficiency is achieved.

References

[1] F. Pellitteri, V. Boscaino, A. O. Di Tommaso, F. Genduso and R. Miceli, "E-bike battery charging: Methods and circuits," 2013 International Conference on Clean Electrical Power (ICCEP), Alghero, Italy, 2013, pp. 107-114, doi: 10.1109/ICCEP.2013.6586975.

[2] R. Yu, T. Chen, P. Liu and A. Q. Huang, "A 3-D Winding Structure for Planar Transformers and Its Applications to LLC Resonant Converters," in IEEE Journal of Emerging and Selected Topics in Power Electronics, vol. 9, no. 5, pp. 6232-6247, Oct. 2021, doi: 10.1109/JESTPE.2021.3052712.

[3] R. Chen, P. Brohlin and D. Dapkus, "Design and magnetics optimization of LLC resonant converter with GaN," 2017 IEEE Applied Power Electronics Conference and Exposition (APEC), Tampa, FL, USA, 2017, pp. 94-98, doi: 10.1109/APEC.2017.7930678.

[4] C. Yan, F. Li, J. Zeng, T. Liu and J. Ying, "A Novel Transformer Structure for High power, High Frequency converter," 2007 IEEE Power Electronics Specialists Conference, Orlando, FL, USA, 2007, pp. 214-218, doi: 10.1109/PESC.2007.4341991.

[5] C Z. Ouyang and M. A. E. Andersen, "Overview of Planar Magnetic Technology—Fundamental Properties," in IEEE Transactions on Power Electronics, vol. 29, no. 9, pp. 4888-4900, Sept. 2014, doi: 10.1109/TPEL.2013.2283263.

[6] Zhang, Jun. "Analysis and design of high frequency gapped transformers and planar transformers in LLC resonant converters." ARAN 06/2016 (2015).

[7] Finite Element Method Magnetics 4.2. Available online: http://www.femm.info/wiki/HomePage (accessed on 20 November 2019).